PERIODICO di MINERALOGIA
established in 1930

Dipartimento
di Scienze della Terra
Sapienza
Università di Roma

An International Journal of
Mineralogy, Crystallography, Geochemistry,
Ore Deposits, Petrology, Volcanology
and applied topics on Environment, Archaeometry and Cultural Heritage

A continuous threat: detection of unusual salt phases on the painted wall reliefs of Khonsu temple at Karnak complex, Egypt: a case study

Hussein H. Marey Mahmoud [1,*] and Abdelhakim El-Badry [2]

[1] Department of Conservation, Faculty of Archaeology, Cairo University, Giza 12613, Egypt
[2] Ministry of Tourism and Antiquities, Luxor, Egypt

ARTICLE INFO

Submitted: October 2021
Accepted: February 2022
Available on line: February 2022

* Corresponding author:
marai79@cu.edu.eg

Doi: 10.13133/2239-1002/17608

How to cite this article:
Marey Mahmoud H.H. and El-Badry A. (2022)
Period. Mineral. 91, 47-61

ABSTRACT

Salt damage is a dominant threat to the ancient monuments in Upper Egypt. This study investigates unusual salt phases formed on the painted wall reliefs of Khonsu temple at the Karnak complex. Optical and petrographic examinations observed the main characteristics of stone, plasters and salt encrustations. High-resolution field emission scanning electron microscope (HR-FESEM) -together with its microanalyzer- and X-ray diffraction analysis (XRD) have successfully revealed the microstructure, chemical and mineralogical phases of the studied samples. The Fourier transform infrared spectroscopy (FTIR) evaluated the molecular structure of some samples. The analyses revealed salt minerals that frequently crystallize on stone monuments such as calcium sulphates (gypsum $CaSO_4 \cdot 2H_2O$, bassanite $CaSO_4 \cdot 0.5H_2O$ and anhydrite $CaSO_4$), calcium carbonate (calcite polymorph, $CaCO_3$), and halite (NaCl). While, unusual salt phases of urea $CO(NH_2)_2$ and archerite $(K,NH_4)(H_2PO_4)$ have been identified. The two latter minerals have not been previously reported on similar monuments in Egypt. By observing the studied temple, a possible hypothesis for salt formation was proposed. It is strongly suggested that the bat guano accumulated on the temple walls is the major cause. Thus, the produced nitrogen and phosphorus-based chemicals stimulate a severe damage to the sandstone reliefs and in consequence, the formation of salt crystals. While, the additional salt minerals are highly associated to the combination of several weathering processes.

Keywords: Khonsu temple at Karnak; Painted wall reliefs; Salt weathering; HR-FESEM/EDX; XRD; Urea; Archerite; Bat guano.

INTRODUCTION

Environmental impacts are acting aggressively to produce a measurable damage to the cultural heritage structures (Steiger, 2003; Gómez-Heras et al., 2004; El-Gohary, 2010; Marey Mahmoud et al., 2010; El-Gohary and Abdel Moneim, 2021). Wall paintings and reliefs are exposed to extensive daily and seasonally environmental variations (e.g. air temperatures, relative humidity, etc.). Furthermore, microbiological activities on stone materials induce several forms of damage. The components of wall paintings provide necessary nutrients for colonizing several microorganisms. Consequently, routes of chemical processes are occurred and therefore, aesthetic biofilms are expected (Guglielminetti et al., 1994; Unković et al., 2016; Liu et al., 2020). But, the most hazardous effect is attributed to the crystallization of salts. Among the salt types that were detected on the ancient Egyptian monuments, sodium chloride (halite, NaCl) and calcium sulphate phases (gypsum $CaSO_4 \cdot 2H_2O$, bassanite $CaSO_4 \cdot 0.5H_2O$, anhydrite $CaSO_4$) are the most common ones. These salt minerals have been previously analyzed in many monuments such as Hibis temple at Kharga Oasis of the Western Desert (Hosam and Kamh, 2016), Karnak temples complex (Martinet et al., 1992; Marey Mahmoud et al., 2010; Abd-Elkareem, 2014), Esna temple (Bader, 2014) and in the Nobles tombs at Luxor (Wüst and Schülchter, 2000; Marey Mahmoud, 2010). More, El-Gohary (2016) has identified sylvite (KCl) and thenardite (Na_2SO_4) as major salts present in the temple of Horus at Edfu, Upper Egypt. According to Arnold and Zhender (1987), salts are usually occurred as surface deposits or as growing crystals inside the stone microstructure. In addition, saline solutions are distributed into the pore matrix. Basically, building materials, air pollution, microorganisms and groundwater are the main suppliers for salt ions (Megahed, 2020). In certain cases, sulphate and phosphate minerals can be accomplished due to the reactions of bat guano (Hosono et al., 2006).

Indeed, there is an agreement in the literature that salts exert both hydration and crystallization pressures. The low evaporation rate, compared to the solution rate, enhances the crystallization of soluble salts on stone surfaces (Salman et al., 2010). On the contrary, the high evaporation rate will lead to the formation of salts within the inner pore structure (Scrivano and Gaggero, 2020). According to Cardell et al. (2003), the crystallization of salts decreases stone durability through increasing its total porosity and pore size distribution. Thus, cycles of crystallization and re-dissolving of salts will produce destructive effects on the building materials. As concluded by La Russa et al. (2013), the deterioration of stone is highly attributed to the high crystallization pressure and small pores. As follows, salt crystals will activate exfoliation, blistering and the disintegration of stone. Although the majority of previous studies did not observe any phosphate-based minerals on the ancient Egyptian monuments, Bakr and Abd El Hafez (2012) reported minerals of brushite [$Ca(PO_3OH \cdot 2H_2O$], whitlockite [$Ca_9Mg(PO_3OH)PO_4)_6$] and newberyite [$MgPO_3OH) \cdot 3H_2O$] on 19^{th} century decorations at the city of Suez of Egypt. The authors concluded that biodeterioration is responsible for the occurrence of the mentioned salts.

In the present approach, morphological, mineralogical and spectroscopic methods were conducted to explain the source of some encrustations formed on the wall reliefs of Khonsu temple at Karnak complex, Upper Egypt. The samples were analyzed using several analytical methods included USB digital optical microscope, high-resolution field emission scanning electron microscope (HR-FESEM) with a microanlayzer spectrometer, X-ray diffraction analysis (XRD) and Fourier transform infrared spectroscopy (FTIR). Based on that, unusual nitrogen and phosphate-rich compounds were measured. As urea and archerite have never been previously identified on ancient Egyptian monuments, thus, highlighting their possible source and their responsibility for the deterioration process of the temple were considered the main objectives of this study.

The studied site

Khonsu temple is a complete structure, to some extent, which dates back to the New Kingdom of ancient Egypt (ca. 1550-1070 BC). This temple is located at the South-Western section of the Karnak complex. It comprises many minor structures including side decorated chapels. Based on the great importance of Karnak, several studies have been contributed to understand the weathering processes affecting on the site (of them are: Billard and Burns, 1980; Ismail and Abdel Moniem, 1999; Simon and Lind, 1999; Marey Mahmoud et al., 2010; Mansour and El Attar, 2019). In the studied site, signs of bat droppings and two surface encrustations were recorded. The first encrustation represents stalactite formations, while the second is a thick superficial crust.

Metrological data of the studied site

The reports of the Egyptian Meteorological Centre (EMC) referred that Luxor climate is described as arid and semi-arid desert (Ahmed and Fogg, 2014). During the summer season, the air temperature reaches 44 °C, while during winter months it shows 32 °C. The relative humidity (RH%) reports 50% in December, and in August, it gives a value of 29%. The lowest evaporation value (2.5 mm/day) is usually registered in January, while the highest rate is reported in June (9.4 mm/day) (EL-Bayomi, 2007). Basically, different salt types are crystallized, depending on the saline solution itself and the surrounding environmental conditions such as the air temperature and RH% (Oguchi and Yu, 2021). According to Arnold and Zehnder (1989), the periodic crystallization of salts is highly influenced by the seasonal variations in air temperatures. The metrological data show that the studied area has low precipitation and high evaporation rate which accelerate the movement of moist out of pores and therefore, salts are crystallized on the surface of stone.

METHODOLOGY

Samples

As observed in Figure 1, salt encrustations and wasp nests are deposited on the painted reliefs of the studied temple (Chapel No. 2). Actually, the removal of salt encrustations and similar deterioration forms is a desirable request for any restoration project. Taking into consideration the underlying paint layers, several fractions from the encrustations were removed. Subsequently, four representative samples (with different dimensions) have

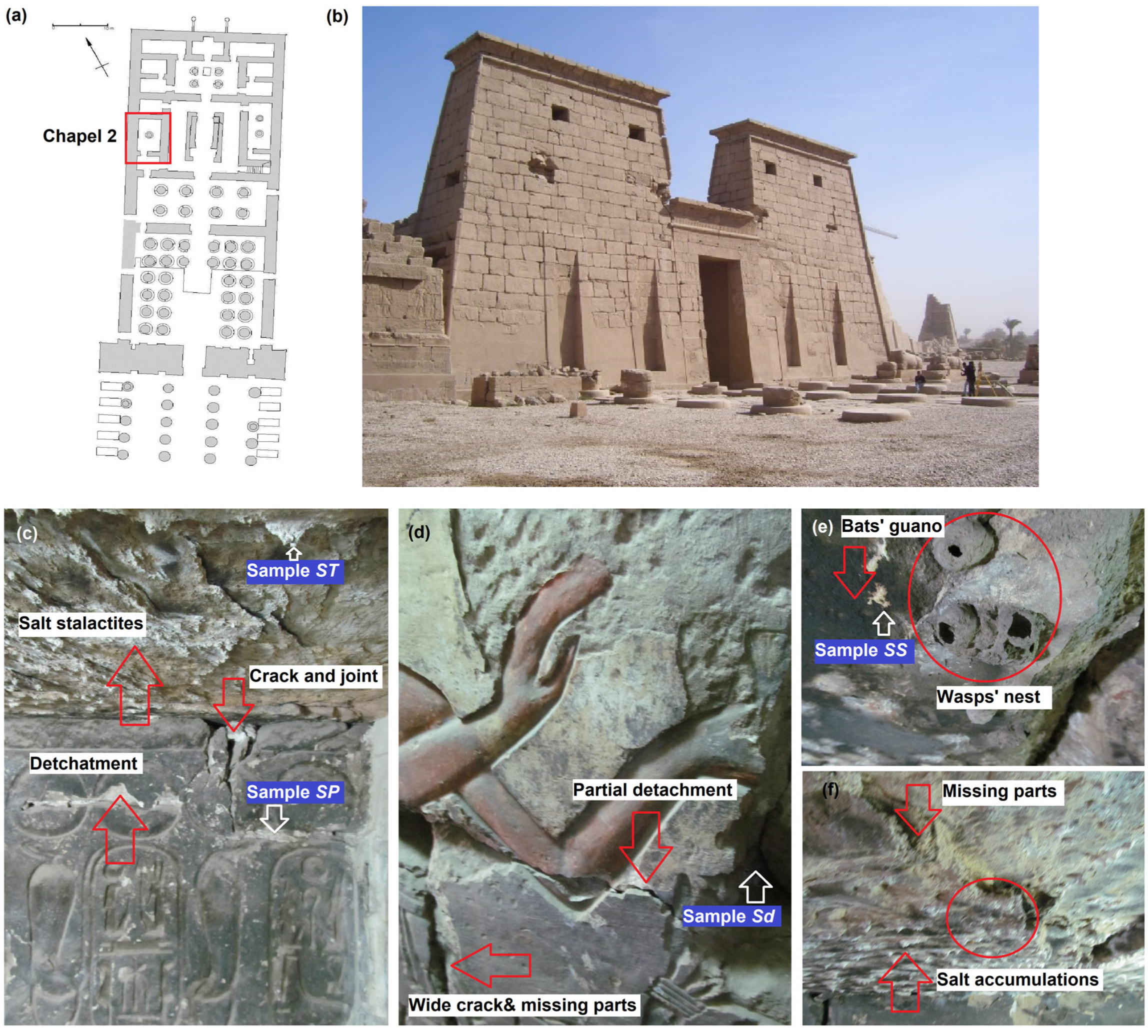

Figure 1. (a) A schematic plan of Khonsu temple at the Karnak complex (Chapel No. 2 is highlighted with a red rectangle), (b) An overview view of the temple, (c-f) Examples on the deterioration forms on the painted wall reliefs of the temple.

been analyzed by a number of analytical methods. Table 1 shows a brief description of the studied samples.

Analytical methods

Initially, the samples were checked by a digital mobile USB microscope "dnt Co., Germany". The microscope is supported by a digital camera (5.0 megapixel) and magnifications between 10x to 500x. More, the petrographic tests on stone and plaster layers were applied using a Nikon polarized light microscope (model: "Eclipse-E600"). Petrographic analysis extends useful description of the geological nature of samples and any deformation of minerals. The instrument is attached to a high-resolution digital camera (model: "PixeLINK PL-A623"). As a basic method for characterizing the morphological structure of samples, a high-resolution field emission scanning electron microscope (model: "Philips Quanta FEG 250", operated at 20 kV accelerating voltage) was used. The chemical composition of the samples was measured using an EDX analyzer. To measure the mineral phases, the deterioration products were pulverized to a fine powder which then was analyzed using X-ray diffractometer (model: PANalytical "PW3040/60 X'Pert PRO"). The diffractometer was operated using a Cu-K$_\alpha$ radiation source at wavelength of 1.54060 Å. The XRD patterns were obtained on a range of 0-60° (2θ). The operating conditions were: 40 kV (power) and 30 mA (current). Mineral identification was available using a Match! Phase analysis software aided with "COD- reference REV120941database". Calculating the percentages of the crystalline minerals for each sample was performed through the "QXRD-

Table 1. Description of the studied samples from the Chapel No. 2, Khonsu temple.

Sample code	No. of samples	Location	Description
Sd	2	The northwest wall of the chapel	Sandstone fragments (with approx. dimensions of 1.5 ×2 cm^2)
SS	3	Left Upper corner of the chapel	Salt encrustations formed on the stone walls (with approx. dimensions of 2×3.5 cm^2)
SP	2	Higher zone of the south wall	Salt encrustations formed on the plaster layers (with approx. dimensions of 1.5×3 cm^2)
ST	4	Ceiling of the chapel	Salt encrustations from the stalactite formations on the ceilings

Rietveld method". Further, portions of the collected encrustations were analyzed by Fourier transform infrared spectrophotometer (model: "JASCO FT-IR 4100"). The transmittance spectra were obtained over a typical mid-IR spectral region (4000-400 cm^{-1}) using a resolution of 4 cm^{-1} supported with 32 scans per each spectrum.

RESULTS AND DISCUSSION

Microscopic features

Figure 2 highlights optical images achieved on the studied samples. The examination of a weathered sandstone (Sample *Sd*) displayed quartz grains, with different dimensions, are blended with soot particulates (Figure 2a). For the sample (*SS*), several salt crystals were observed (Figure 2b). The sample (*SP*) appeared as a friable structure which is covered with a black layer (with a uniform thickness from 100 to 250 µm) (Figure 2c). The examination of stalactite formations (Sample *ST*) reveals salt crystals and large siliceous grains (Figure 2d).

Petrographic observation

Figure 3 shows photomicrographs of sandstone and plaster samples, under plane and crossed- polarized light. The petrographic observation of the sandstone sample showed constituents of fine monocrystalline angular and subrounded quartz grains along with few amounts of polycrystalline quartz. In the section below, X-ray diffraction analysis of the sample showed major peaks of quartz which suggest the stone type as siliceous quartz arenite (Temraz and Khallaf, 2016). This sandstone type contains fine quartz grains with an average size from 0.06 mm to 2 mm. In this stone, the cementation between grains is occurred through silica or quartz cement overgrowth. However, iron oxides may also present as a filler for the secondary pores which distinguishing the Nubian sandstone type (El-Gohary and Radwan, 2018). Probably, these iron oxides are the result of 'in-place' alteration of iron-rich minerals (Zaid et al., 2018). According to Prajapati et al. (2020), the polycrystalline sandstone has a lower quartz cement than the monocrystalline one. In order to treat the wall defects, the reliefs were covered with a plaster layer made of gypsum with minor amounts of calcite and few portions of quartz. The petrographic observation of the plaster layer revealed a heterogeneous texture filled with fine carbonatic grains and bright gypsum veins. Over the above, quartz grains are observed in the section.

Morphological-microanalysis and mineralogical analysis (FE-SEM/EDX & XRD)

Table 2 and Table 3 extract the EDX and XRD results of the studied samples.

Sandstone (Sample *Sd*)

The ancient Egyptians used durable building materials for their constructions. The sandstone sample (*Sd*) showed a notable friability and it was easily crushed by hand. The FE-SEM image of the sample shows etched and eroded quartz grains (Figure 4, Up). Bright crystals of the iron oxides cementation are also observed. More, the investigation showed the distribution of several agglomerations, probably of clay minerals. A bulk EDX measurement on the sample proved the presence of silicon (Si, 11.33%) and iron (Fe, 23.23%) (Figure 4, Bottom). Elements of aluminium (Al, 3.55%), magnesium (Mg, 1.36%), calcium (Ca, 0.9%), and chlorine (Cl, 0.86%) were also determined in the spectrum. X-ray diffraction analysis was performed to identify the main crystalline phases included in the sample. By analyzing the pattern, a prominent percentage of quartz (SiO_2) was measured (Figure 5). In contrast to EDX results, the XRD pattern did not show any minerals of iron oxides, this probably due to the detection limit of the diffractometer. Harrell (2016) demonstrated that SiO_2, Fe-oxides, $CaCO_3$, and

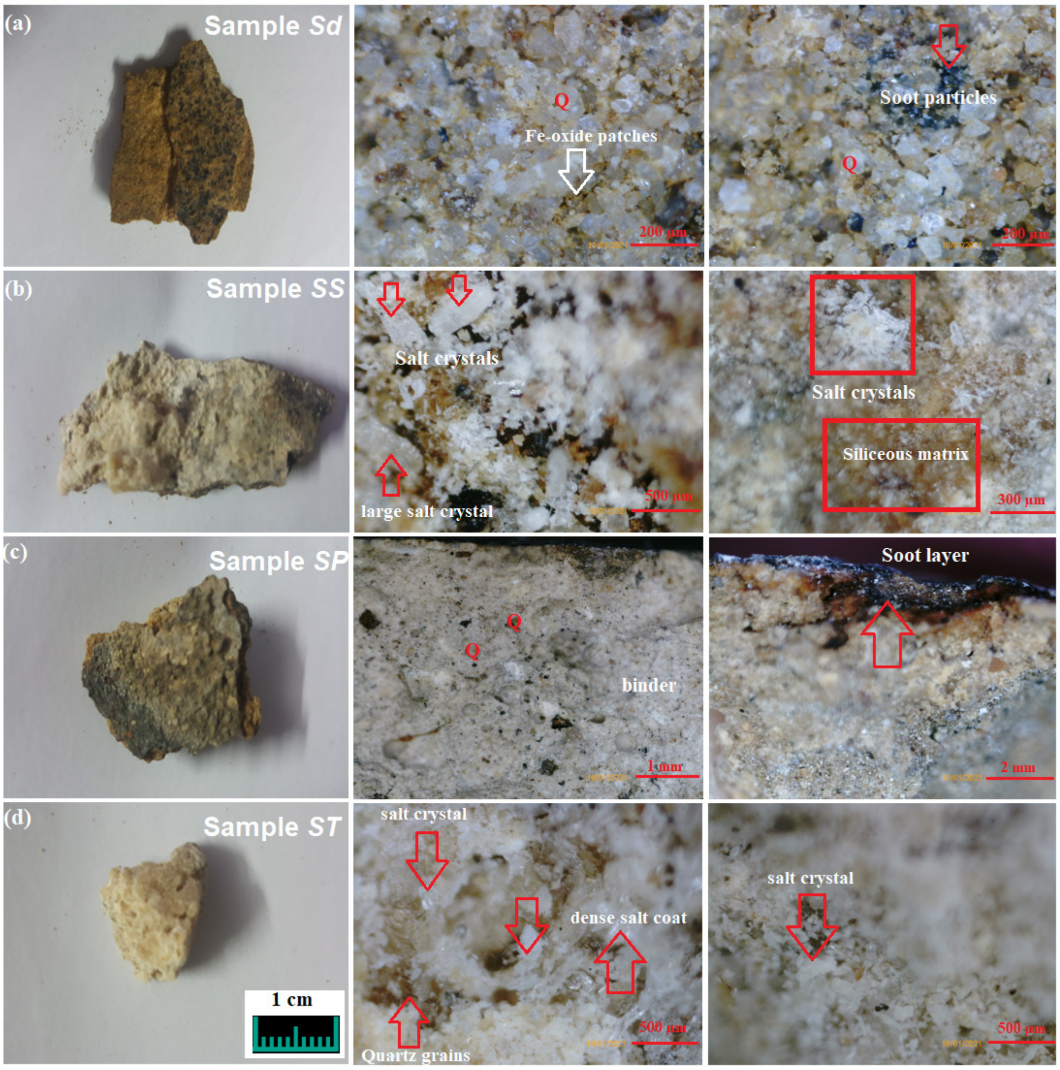

Figure 2. View of the studied samples (Left) and microscopic images obtained by USB digital microscope on the samples (Right).

clay minerals are frequently contained as cementing materials in sandstones.

Salt encrustation on stone walls (Sample *SS*)

The FE-SEM image of a salt encrustation (Sample *SS*) provided interesting microstructural aspects (Figure 6a). As noticed in the centre of the micrograph, accumulations of micro-sized subhedral crystals are found. EDX scans of this area showed variable concentrations of sulphur (S, 6.16%), potassium (K, 6.95%), phosphorus (P, 3.15%), nitrogen (N, 13.46%), calcium (Ca, 4.56%), and sodium (Na, 2.57%) (Figure 7, Up). In Figure 6b, white fine grains are observed. The nitrogen high atomic concentration is associated with the presence of nitrogen-containing compounds, most likely resulting from biochemical processes (Li et al., 2021). The XRD pattern recorded on the sample showed minerals of urea [($CO(NH_2)_2$, 93%] and archerite [($(K,NH_4)(H_2PO_4)$, 7%] (Figure 8).

Crystallization of urea

Regrettably, bat colonies that usually occupy the higher sections of the temples in Upper Egypt are genuine problems for conservators. The droppings and excrete of bats deform the aesthetic values of the reliefs and they supply sufficient nutrients for the microbial growth (Singh and Gupta, 2020). More, these deposits may produce additional physical damage to the painted surfaces. Biologists reported that bats excrete nitrogen-rich compounds of uric acid and urea. Urea comprises the main component of bat's urine with a percentage of 70%.

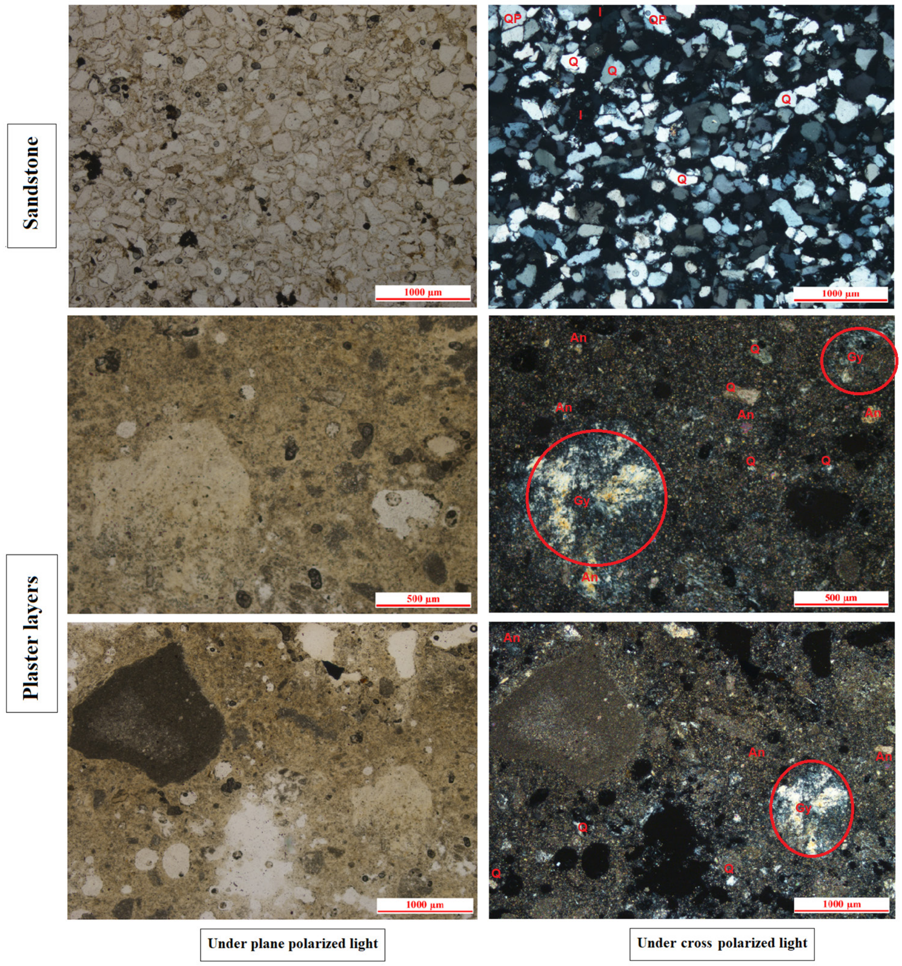

Figure 3. Photomicrographs on stone and plaster samples, under plane and crossed- polarized light. Q=Monocrystalline quartz; QP= Polycrystalline quartz; I= Iron oxides; An=Anhydrite; Gy=Gypsum.

Table 2. EDX microanalysis (wt% and at%) of the studied samples.

Elm.	Sample *SD*		Sample *SS*		Sample *SP*		Sample *ST*	
	wt%	at%	wt%	at%	wt%	at%	wt%	at%
C	-	-	11.49	18.49	14.78	21.94	18.76	25.13
N	-	-	9.75	13.46	14.16	18.03	26.43	30.35
O	34.18	58.77	36.94	44.65	39.93	44.5	34.77	34.95
Na	-	-	3.05	2.57	1.55	1.20	1.27	0.89
P	-	-	5.05	3.15	-	-	5.91	3.07
Mg	1.20	1.36	-	-	1.02	0.75	-	-
Al	3.49	3.55	-	-	-	-	-	-
Si	11.57	11.33	-	-	1.44	0.91	0.36	0.21
S	-	-	10.22	6.16	4.05	2.25	3.1	1.56
Cl	1.10	0.86	-	-	2.28	1.15	-	-
Ca	1.31	0.9	9.46	4.56	19.5	8.67	1.76	0.71
Fe	47.15	23.23	-	-	-	-	-	-
K	-	-	14.05	6.95	1.29	0.59	7.63	3.14

Table 3. The crystalline mineral phases measured by XRD method on the studied samples.

Crystalline phase	IMA mineral formula	Reference code	Sample SD	Sample SS	Sample SP	Sample ST
Quartz	SiO_2	[96-901-5023]	+++	–	+	+
Urea	$CO(NH_2)_2$	[96-100-8786]	–	+++	–	–
Archerite	$(K,NH_4)(H_2PO_4)$	[96-900-7431]	–	++	–	++
Calcite	$CaCO_3$	[96-101-0929]	–	–	+++	+++
Gypsum	$CaSO_4{\cdot}2H_2O$	[96-901-5351]	–	–	++	+++
Anhydrite	$CaSO_4$	[96-900-4097]	–	–	++	++
Bassanite	$CaSO_4{\cdot}0.5H_2O$	[96-901-5437]	–	–	+	++
Halite	NaCl	[96-900-8679]	–	–	++	+

– = not determined; + = traces; ++ = minor constituent; +++ = major constituent.

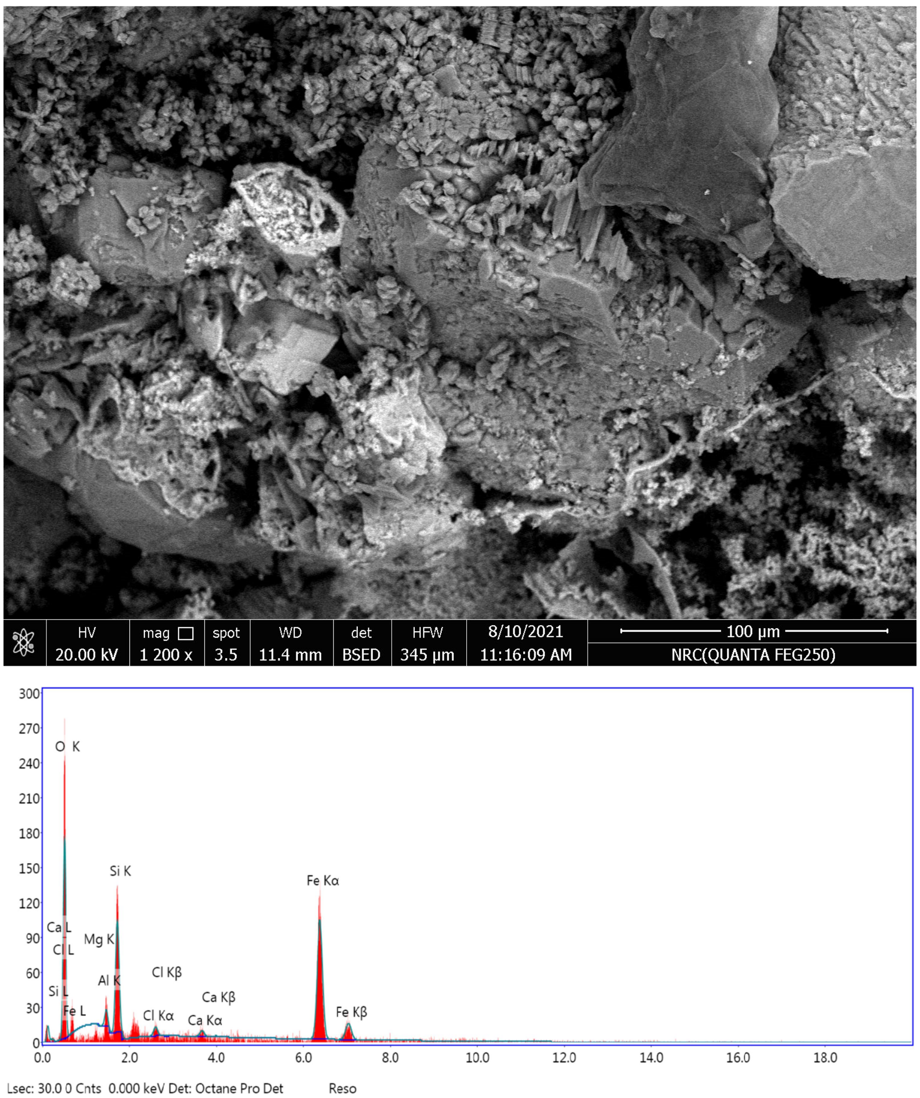

Figure 4. (Up): FE-SEM image -in the backscattered electron mode (BSE) (1200×, scale bar = 100 μm),- and (Bottom): EDX spectrum recorded on the sandstone sample.

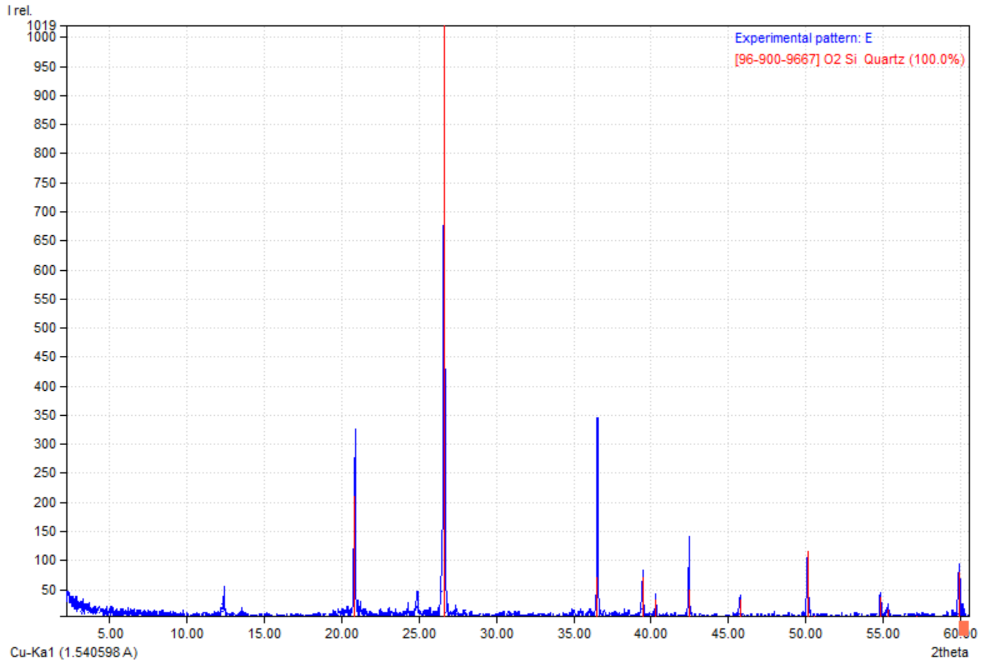

Figure 5. X-ray diffractogram of the sandstone sample.

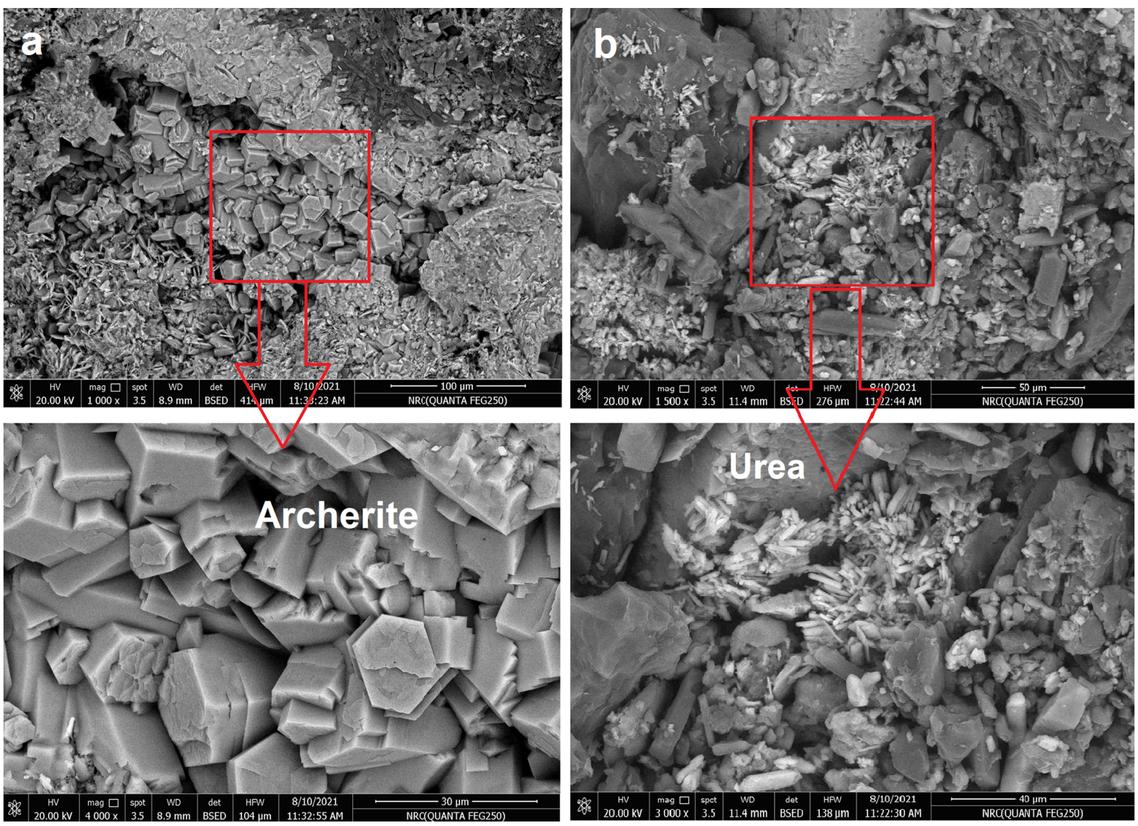

Figure 6. FE-SEM micrographs -in the backscattered electron mode (BSE)- collected on a salt encrustation formed on the stone walls (Sample SS), (a) archerite crystals (Up: 1000×, scale bar =100 µm, Bottom: 4000×, scale bar = 30 µm), (b) urea crystals (Up: 1500×, scale bar = 50 µm, Bottom: 3000×, scale bar = 40 µm).

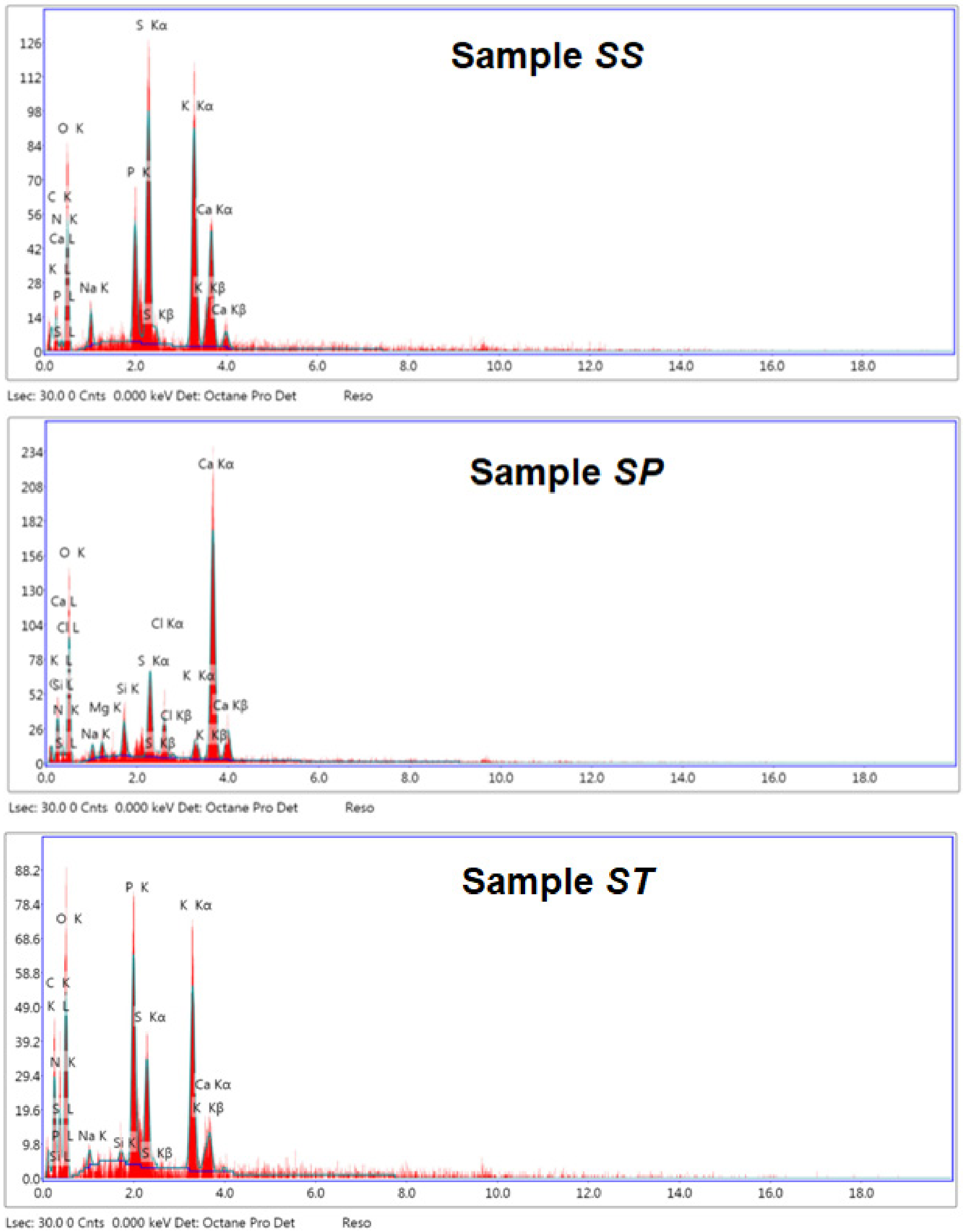

Figure 7. EDX spectra collected on the samples (SS, SP, ST).

As described by Audra et al. (2017), the formation of urea begins through the catabolism process which produces amounts of H_2O and CO_2, in addition to nitrogenous compounds. Then, ammonia (NH_3) is formed due to the breakdown of amino acids, which thereafter, reacts with CO_2 to form urea. When the relative humidity (RH) in the surrounding environment is below 68%, the produced urea will crystallize as salt (Ellewsen, 2019). Effectively, the dry conditions of the studied area facilitate the crystallization of urea and several salts.

Crystallization of archerite

Further, phosphorus and archerite were measured in the same sample, through the EDX and XRD techniques, respectively. Archerite, also known as 'biphosphammite', is a phosphate mineral associated to bat guano deposits that frequently occur in caves. Bat guano, or the excreta of bats, is essentially composed of about 25% phosphate with constituents of sulphate and a wide group of ions including K, NH^{4+}, Na, Mg, Ca, P, Al, and Fe (Sakoui et al., 2020). Commonly, archerite is formed through the

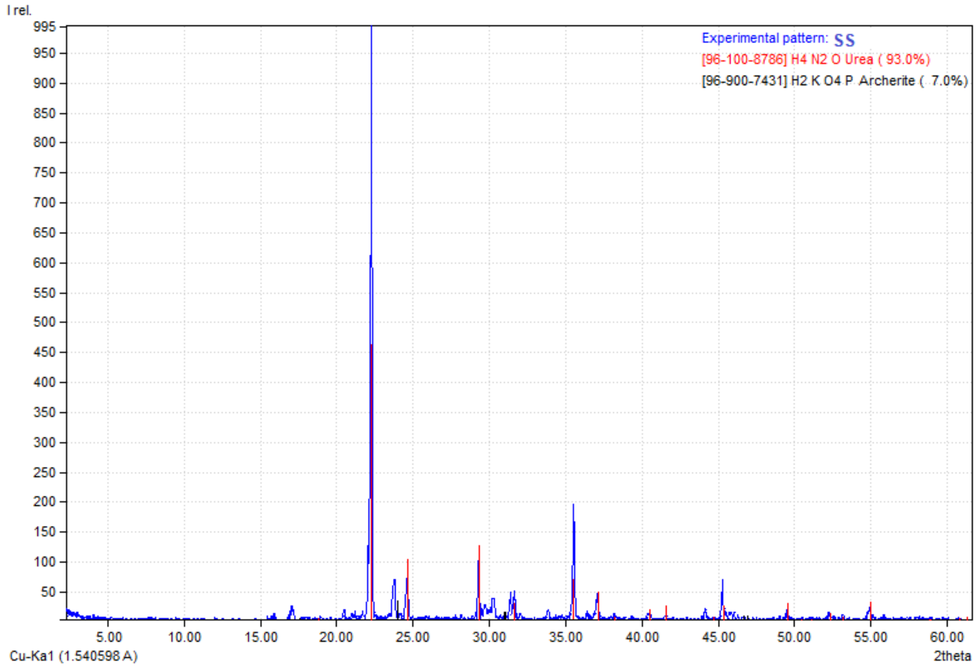

Figure 8. X-ray diffractogram obtained on the sample (SS), crystalline phases of urea and archerite were measured.

reaction of bat guano water-soluble chemicals, which then, will participate on the stone surface (Frost et al., 2012). Otherwise, it can be produced through the direct contact of the chemicals mentioned above with the stone material. It is said that bat guano, in combination with sulphur-oxidizing bacteria, provides several amounts of P_2O_5 and SO_3 (Uchida et al., 1999). Further, Birch (2005) reported that phosphate minerals are originated through leaching out the soluble nitrogen from the guano and leaving the phosphorus ions behind. Then, phosphorus combines with the cations released from the stone matrix to produce new compounds. This reaction is favourable in a warm weather linked with high evaporative conditions. Under these factors, potassium and phosphorus are moving from the bat guano and they crystallize as salts (Onac et al., 2009). Additionally, the irrigation water in the nearby area has affected negatively the quality of the groundwater by adding another source of potassium (K^+) and phosphate ions (PO_4^{3-}).

Salt encrustation on plaster layers (Sample *SP*)

The morphological illustration of a salt encrustation formed on the plaster layers (Sample *SP*) is given in Figure 9a. The FE-SEM micrograph shows the distribution of dense biofilms and filaments. Chaudhary and Goyal (2019) reported that the common microflora in arid conditions are the mineral oxidising fungi, e.g. sulphur compounds. An EDX spectrum of the sample unveiled calcium (Ca, 8.67%), nitrogen (N, 18.03%), sodium (Na, 1.20%), magnesium (Mg, 0.75%), silicon (Si, 0.91%), sulphur (S, 2.25%), chlorine (Cl, 1.15%), and potassium (K, 0.59%) (Figure 7, Middle). The XRD pattern of the sample revealed peaks of calcite ($CaCO_3$, 43.3%), gypsum ($CaSO_4 \cdot 2H_2O$, 27.2%), anhydrite ($CaSO_4$, 15.1%), bassanite ($CaSO_4 \cdot 0.5H_2O$, 10.8%), quartz (SiO_2, 2.1%), and halite (NaCl, 1.5%) (Figure 10).

It is possibly that the penetration of the groundwater allows the formation of calcium sulphate salts. Worthy to note that the soil salinity of the Egyptian lands has been affected after the construction of the Aswan High Dam (Benedick, 1979). By analyzing groundwater samples from the studied area, salt ions of carbonate, bicarbonate, chloride, sulphate, and nitrate were detected (Megahed, 2020; Said et al., 2021). Subsequently, salt ions are transferred into the foundations under the temple, then they penetrate into the walls by the capillary rise. As a result and depending on the surrounding climatic conditions, several salt minerals are crystallized. In their field study at Karnak temples, El-Gohary and Redwan (2018) concluded that the weathering of the stone sculptures in the site is highly linked to the groundwater. In addition, the authors demonstrated that halite (NaCl), sylvite (KCl), bischofite ($MgCl_2 \cdot 6H_2O$) are the dominant salt types in the site. The crystallization of gypsum in monuments, calcium sulphate dihydrate, commonly requires a high water content (Galvan lopis et al., 1992;

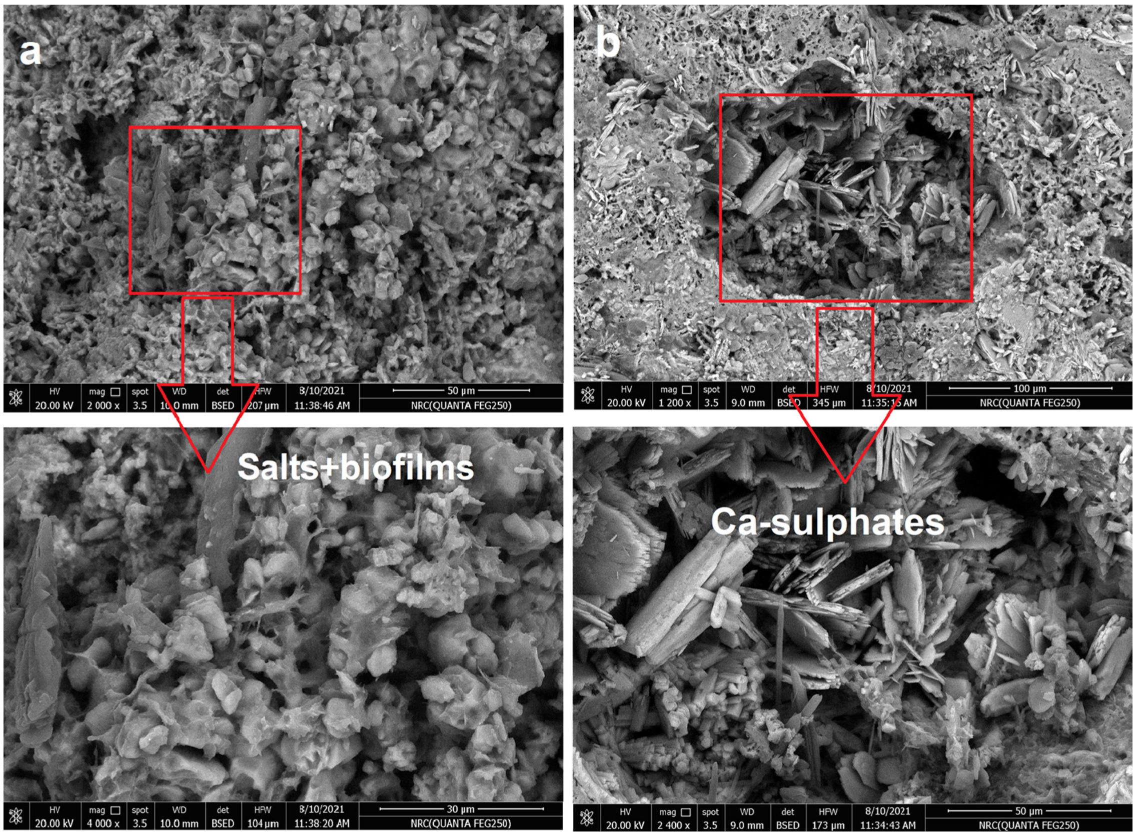

Figure 9. FE-SEM micrographs -in the backscattered electron mode (BSE)- collected on: (a) salt encrustation formed on the plaster layers (Sample SP) (Up: 2000×, scale bar = 50 µm, Bottom: 4000×, scale bar =30 µm), (b) salt encrustation from the stalactite formations on the ceilings (Sample ST) (Up: 1200×, scale bar = 100 µm, Bottom: 2400×, scale bar = 50 µm).

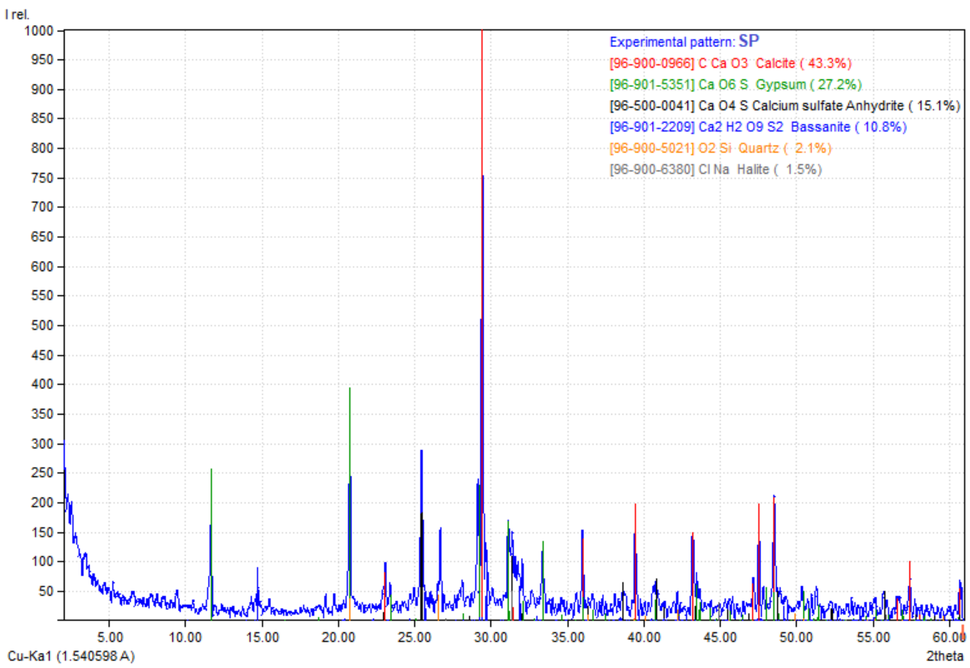

Figure 10. X-ray diffractogram of the sample (SP) revealed minerals of calcite, gypsum, anhydrite, bassanite, quartz and halite.

Zehnder, 2007). In the higher zones of the temple walls, the existence of gypsum salts is strongly combined with hygroscopic salts, e.g. NaCl (Zehnder, 1996; Charola et al., 2007). Certainly, NaCl was measured through the XRD analysis of the studied sample. Apparently, it was reported that the conversion of gypsum into hemihydrates or anhydrous phases requires high temperatures (Mees and De Dapper, 2005). Obviously, the arid conditions of the studied area motivate the dehydration process. Furthermore, Audra et al. (2019) declared that gypsum may crystallize as by-product due to the effect of bat guano.

Salt encrustation from the stalactite formations (Sample *ST*)

The morphological study of salt encrustation from the stalactite formations on the ceilings of the temple (Sample *ST*) showed characteristic calcium sulphate crystals (Figure 9b). The images showed platy and prismatic crystals with fibrous aggregates. The EDX microanalysis of these crystals showed elements of nitrogen (N, 30.95%), sodium (Na, 0.89%), phosphorus (P, 3.07%), silicon (Si, 0.21%), calcium (Ca, 0.71%), and potassium (K, 3.14%) (Figure 7, Bottom). XRD analysis of the sample showed significant minerals of calcite and gypsum with a minor existence of anhydrite, bassanite and archerite. Quartz and halite were also measured in a small quantity. Bakr and Abd El Hafez (2012) explained that the presence of P and N is strongly related to the effect of bat guano. Sufficiently, the identification of phosphate and sulphate-based minerals on stone monuments under arid conditions has been previously reported (Uchida et al., 1999).

FTIR results

Infrared spectroscopic analysis was applied to identify the marked functional groups of samples. Figure 11 shows the FTIR spectra collected on some encrustations.

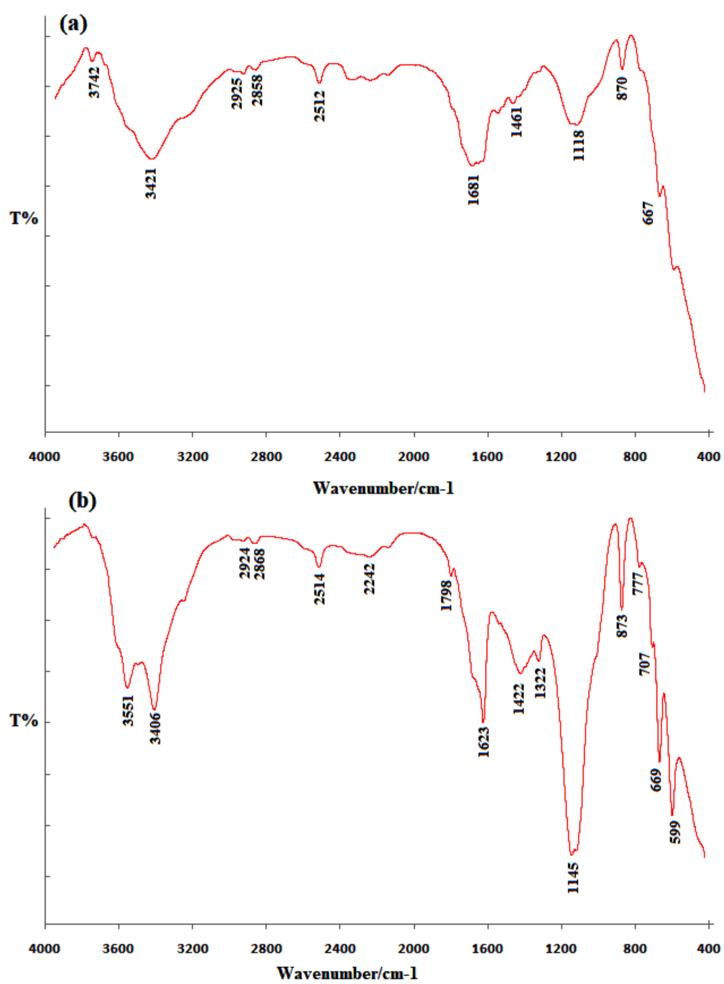

Figure 11. Transmittance FTIR spectra (in the mid-infrared region) acquired on: (a) Sample (SS), (b) Sample (SP).

The FTIR spectrum acquired on the sample (*SS*) is shown in Figure 11a. There were indications on the presence of urea salts through the peaks at 1681 (C=O stretching frequency), 3421 and 1625 cm^{-1} (N-H bending modes). While a C-N stretching vibration was reported at 1461 cm^{-1}. The band related to Si-O-Si asymmetric stretching is noticed at 667 cm^{-1}, while the band at 1118 cm^{-1} is for the C-O-C stretching. In Figure 11b, the spectrum of the sample (*SP*) showed two major sulphate bands at 1623 and 3406 cm^{-1}. The carbonate group was observed at 873, 1145, 1422, 1798 and 2514 cm^{-1}. Quite, the molecular analysis of samples helped to confirm some results that previously obtained through the EDX and XRD techniques.

CONCLUSIONS

The present work was directed to monitor the state of conservation of the painted wall reliefs of Khonsu temple at Karnak complex, Upper Egypt. This scientific approach allowed the identification of several salt accumulations on the painted reliefs. Characterization of samples was performed through extensively used analytical methods (e.g., OM, PLM, FE-SEM/EDX, XRD, FTIR). The analyses proved the occurrence of a group of crystalline salt minerals. Unexpectedly, unusual salt phases such as urea and archerite were reported. Moreover, halite and calcium sulphate phases were also measured. It was concluded that bat guano plays the major role in the formation of some salts. The crystallization of urea is highly related to the bat's urine, in the availability of convenient relative humidity (RH). The formation of archerite is associated to the chemicals released by the bat guano. Quite, the combination of several environmental factors contributes in the formation of the measured salts. Certainly, the penetration of the groundwater beneath the temple walls stimulates the crystallization of different salt species. Necessarily, the protection of the archaeological sites form the negative impacts of bats is a complicated urgent challenge. Importantly, the decision requires the contribution of several authorities taking into consideration both the ecological and heritage perspectives.

ACKNOWLEDGEMENTS

Authors are grateful to the conservators at Karnak temples for their kind support. Also, our sincere thanks to the anonymous reviewers for their constructive comments and suggestions that substantially helped to improve the manuscript.

REFERENCES

Abd-Elkareem E., 2014. Environmental deterioration and conservation of Ramses III's Sandstone Temple, Karnak, Luxor. Journal of the Faculty of Archaeology, South Valley University 9, 1-17.

Ahmed A.A. and Fogg G.E., 2014. The impact of groundwater and agricultural expansion on the archaeological sites at Luxor, Egypt. Journal of African Earth Sciences 95, 93-104. doi: 10.1016/j.jafrearsci.2014.02.007.

Arnold A. and Zehnder K., 1987. Monitoring wall paintings affected by soluble salts, The conservation of wall paintings. In: Proceedings of the symposium organized by the Courtauld Institute of Art and the Getty Institute. (Ed.) Sh. Cather, London, July 13-16, 103-135.

Arnold A. and Zehnder K., 1989. Salt weathering on monuments. In: La conservazione dei monumenti nel bacino del Mediterraneo Influenza dell'ambiente costiero e dello spray marino sulla pietra calcarea e sul marmo Atti del I' Simposio internazionale. (Ed.) F. Zezza, Bari, 7-10 giugno, pp. 31-58.

Audra Ph., Bosák P., Gázquez F., Cailhol D., Skála R., Lisá L., Jonášová Š., Frumkin A., Knez M., Slabe T., Hajna NZ., Al-Farraj A., 2017. Bat urea-derived minerals in arid environment. First identification of allantoin, $C_4H_6N_4O_3$, in Kahf Kharrat Najem Cave, United Arab Emirates. International Journal of Speleology 46, 81-92.

Audra Ph., de Waele J., Bentaleb I., Chroňáková A., Krištůfek V et al., 2019. Guano related phosphate-rich minerals in European caves. International Journal of Speleology, 48, 75-105.

Bader N.A., 2014. The deterioration problems of the wall reliefs of Komir temple, Esna, Egypt. Mediterranean Archaeology and Archaeometry 14, 201-219.

Bakr A. and Abd El Hafez M., 2012. Role assessment of bat excretions in degradation of painted surface from Mohamed Ali's palace, Suez, Egypt. Egyptian Journal of Archaeological and Restoration Studies 3, 47-56.

Benedick R.E., 1979. The High Dam and the Transformation of the Nile. Middle East Journal 33, 119-144.

Billard T.C. and Burns G., 1980. Mechanisms of Stalinization of great Temples in Luxor area. Journal the Society for the study of Egyptian Antiques 10, 243-249.

Birch W.D., 2005. Sedimentary Rocks | Phosphates. In: Encyclopedia of Geology. (Eds.) Selley RC., Cocks L.R.M., Plimer I.R., Elsevier, pp. 120-128. doi: 10.1016/B0-12-369396-9/00282-3.

Cardell C., Delalieux F., Roumpopoulos K., Moropoulou A., Auger F., Van Grieken R., 2003. Salt-induced decay in calcareous stone monuments and buildings in a marine environment in SW France. Construction and Building Materials 17, 165-179.

Charola A.E., Puűhringer J.E., Steiger E.M., 2007. Gypsum: a review of its role in the deterioration of building Materials. Environmental Geology 52, 339-352.

Chaudhary S. and Goyal S., 2019. Sulphur oxidizing fungus: A review. Journal of Pharmacognosy and Phytochemistry 8(6), 40-43.

EL-Bayomi G.M., 2007. The Geomorphological Hazards in the Archaeological Area West of Qena Bend. Journal of Applied

Science Research 3, 175-184.

El-Gohary M., 2010. Investigation on limestone weathering of El-Tuba minaret El Mehalla, Egypt: A case study. Mediterranean Archaeology and Archaeometry 10, 61-79.

El-Gohary M.A., 2016. A holistic approach to the assessment of the groundwater destructive effects on stone decay in Edfu temple using AAS, SEM-EDX and XRD. Environmental Earth Sciences 75 (13). doi: 10.1007/s12665-015-4849-x.

El-Gohary M. and Redwan M., 2018. Alteration parameters affecting the Luxor Avenue of the Sphinxes-Egypt. Science of the Total Environment 626, 710-719. doi: 10.1016/j.scitotenv.2017.12.297.

El-Gohary M.A. and Abdel Moneim A.A., 2021. The environmental factors affecting the archaeological buildings in Egypt, "II Deterioration by severe human activities". Periodico di Mineralogia 90(2). doi: 10.13133/2239-1002/17383.

Ellewsen K.M., 2019. Salt damage around a bat roost at Urnes stave church. Master thesis, Department of Archaeology, Conservation and History, University of Oslo.

Galvan lopis V., Mastomas A., Gilbenso E., 1992. Conditions that influence the position and crystallization of salts. In: The 7th international conference on deterioration and conservation of stone. (Ed.) Delgado Rodrigues J., Lisbon, 895-904.

Gómez-Heras M., Benavente D., Buergo M.A., Fort R., 2004. Soluble salt minerals from pigeon droppings as potential contributors to the decay of stone based Cultural Heritage. European Journal of Mineralogy 16, 505-509.

Guglielminetti M., De Giuli M.C., Radaelli A., Bistoni F., Carruba G., Spera G., Caretta G., 1994. Mycological and Ultra Structural Studies to Evaluate Biodeterioration of Mural Paintings. Detection of Fungi and Mites in Frescos of the Monastery of St Damian in Assisi. International Biodeterioration & Biodegradation 33, 269-283.

Harrell J.A., 2016. Varieties and sources of sandstone used in Ancient Egyptian temples. The Journal of Ancient Egyptian Architecture 1, 11-37.

Quantification of Salt Weathering at Hot Deserts and Evaluation of

Hosam I. and Kamh G.M.E., 2016. Reconstruction Rock, Hibis Temple, Kharga Oasis, Western Desert, Egypt. Journal of Arid Land Studies 26, 143-152.

Hosono T., Uchida E., Suda Ch., Ueno A., Nakagawa T., 2006. Salt weathering of sandstone at the Angkor monuments, Cambodia: identification of the origins of salts using sulfur and strontium isotopes. Journal of Archaeological Science 33, 1541-1551.

Ismail B. and Abdel Moniem A.A., 1999. Environmental deterioration of Karnak Temples, Luxor, Upper Egypt. Bulletin of Faculty of Engineering, Assiut University, Egypt 27, 273-302.

La Russa M.F., Ruffolo S.A., Belfiore C.M., Aloise P., Randazzo L., Rovella N., Pezzino A., Montana G., 2013. Study of the effects of salt crystallization on degradation of limestone rocks. Periodico di Mineralogia 82, 1, 113-127. doi: 10.2451/2013PM0007.

Li J., Deng M., Gao L., Yen S., Katayama Y., Gu J-G., 2021. The active microbes and biochemical processes contributing to deterioration of Angkor sandstone monuments under the tropical climate in Cambodia - A review. Journal of Cultural Heritage 47, 218-226. doi: 10.1016/j.culher.2020.10.010.

Liu X., Koestler R.J., Warscheid T., Katayama Y., Gu J-D., 2020. Microbial deterioration and sustainable conservation of stone monuments and buildings. Nature Sustainability 3, 991-1004. doi: 10.1038/s41893-020-00602-5.

Mansour A. and El Attar R.M., 2019. Assessment of Salt Damage Based on Crystallization Test due to High Groundwater Level in Sandstone Monuments, Luxor, Egypt. International Journal of Scientific & Engineering Research 10, 1352-1360.

Marey Mahmoud, H., 2010. Mineralogical and Spectroscopic Characterization of Some Products Resulting from the Weathering Process on the Tomb of Nakht-Djehuty (TT189), Western Thebes, Upper Egypt. Conservation Science in Cultural Heritage 10, 51-70. doi: 10.6092/issn.1973-9494/2310.

Marey Mahmoud H., Kantiranis N., Stratis I., 2010. Salt damage on the wall paintings of the festival temple of Thutmosis III, Karnak temples complex, Upper Egypt. International Journal of Conservation Science 1, 133-142.

Martinet G., Deioye F.X., Le Roux A., 1992. Nature and weathering of the mortars used in the restoration of the Temple of Amon at Karnak (In French), Bull Liaison Lab Pouts Chaussees 182, 21-26.

Mees F. and De Dapper M., 2005. Vertical variations in bassanite distribution patterns in near-surface sediments, southern Egypt. Sedimentary Geology 18, 1225-1229.

Megahed A.H., 2020. Hydrological and archaeological studies to detect the deterioration of Edfu temple in Upper Egypt due to environmental changes during the last five decades. SN Applied Sciences 2, 1952. doi: 10.1007/s42452-020-03560-x.

Oguchi C.T. and Yu S., 2021. A review of theoretical salt weathering studies for stone heritage. Progress in Earth and Planetary Science 8, 32. doi: 10.1186/s40645-021-00414-x.

Onac P.B., Sumrall J., Mylroie J.E, Kearns J.B., 2009. Cave Minerals of San Salvador Island, Bahamas. In: Environmental Sustainability Books. Book 1. (Eds.) Fleury E.S., Chavez T.A., Vacher H.L., University of South Florida, 1-66. http://scholarcommons.usf.edu/tles_pub/1.

Prajapati N., Abad Gonzalez A., Selzer M., Nestler B., Busch B., Hilgers C., 2020. Quartz cementation in polycrystalline sandstone: Insights from phase-field simulations. Journal of Geophysical Research: Solid Earth 125.e2019JB019137.doi: 10.1029/2019JB019137.

Frost R.L., Xi Y., Palmer S.J., Tan K., Millar G.J., 2012. Vibrational spectroscopy of synthetic archerite (K,NH4) H2PO4- and in comparison with the natural cave mineral.

Journal of Molecular Structure 1011, 128 133. doi: 10.1016/j.molstruc.2011.12.013.

Said I., Salman S.A,. Elnazer A.A., 2021. Salinization of groundwater during 20 years of agricultural irrigation, Luxor, Egypt. Environmental Geochemistry and Health 2021. doi: 10.1007/s10653-021-01135-2

Sakoui O., Derdak R., Addoum B., Serrano-Delgado A., Soukri A., El Khalfi B., 2020. The Life Hidden Inside Caves: Ecological and Economic Importance of Bat Guano. International Journal of Ecology 2020. doi: 10.1155/2020/9872532.

Salman A.B., Howari F.M., El-Sankary M.M., Wali A.M., Saleh M.M., 2010. Environmental impact and natural hazards on Kharga Oasis monumental sites,Western Desert of Egypt. Journal of African Earth Sciences 58, 341-353. doi: 10.1016/j.jafrearsci.2010.03.011.

Scrivano S. and Gaggero L., 2020. An experimental investigation into the salt-weathering susceptibility of building limestones. Rock Mechanics and Rock Engineering 53, 5329-5343. doi: 10.1007/s00603-020-02208-x.

Simon S. and Lind A.M., 1999. Decay of limestone blocks in the block fields of Karnak Temple (Egypt): Non-destructive damage analysis and control of consolidation treatments. In: The 12th Triennial Meeting, ICOM committee for Conservation. (Eds.) Bridgland J. and Brown J., Lyon, James and James (Science Publishers), 743-749.

Singh M.R. and Gupta D.A., 2020. Removal of Bats' Excreta from Water- Soluble Wall Paintings Using Temporary Hydrophobic Coating. Journal of the American Institute for Conservation, 1-12. doi: 10.1080/01971360.2020.1734749.

Steiger M., 2003. Crusts and salts. In: The effects of air pollution on the built environment. (Ed.) Brimblecombe P., Air pollution reviews 2, 133-181.

Temraz M.G. and Khallaf M.K., 2016. Weathering behavior investigations and treatment of Kom Ombo temple sandstone, Egypt e Based on their sedimentological and petrogaphical information. Journal of African Earth Sciences 113, 194-204.

Uchida E., Ogawa, Y., Maeda N., Nakagawa T., 1999. Deterioration of stone materials in the Angkor monuments. Cambodia. Engineering Geology 55, 101-112.

Unković N., Ljaljević Grbić M., Stupar M., Savković Z., Jelikić A., Stanojević D., Vukojević J., 2016. Fungal-Induced Deterioration of Mural Paintings: In Situ and Mock-Model Microscopy Analyses. Microscopy and Microanalysis 22, 410-421. doi: 10.1017/S1431927616000544.

Wüst R.A.J. and Schülchter Ch., 2000. The Origin of Soluble Salts in Rocks of the Thebes Mountains, Egypt: The Damage Potential to Ancient Egyptian Wall Art. Journal of Archaeological Science 27, 1161-1172.

Zaid S.M., El-Badry O.A., Abdelaziz Z.A., 2018. Petrography and geochemistry of the Upper Cretaceous Nubia sandstones, Eastern Desert, Egypt: implications for provenance, paleoweathering, and tectonic setting. Arabian Journal of Geosciences 11, 352. doi: 10.1007/s12517-018-3705-1.

Zehnder K., 1996. Gypsum efflorescence in the zone of rising damp monitoring of slow decay processes caused by crystallizing salts on wall paintings. In: The 8th conference on deterioration and conservation of stone. (Ed.) Riederer J., Berlin, 1669-1678.

Zehnder K., 2007. Long-term monitoring of wall paintings affected by soluble salts. Environmental Geology 52, 353-367.